Chapter 7

Study of the glass transition in a Chalcogenide glass

7.1 Introduction

The nature of the glass transition is one 'of the few unsolved problems in condensed matter physics. The primary question is whether the glass transition can be described purely on the basis of a kinetic picture or thermodynamics also plays a role in it. The phenomenon of glass transition has been extensively studied as a function of composition, in multi-component systems []. The effect of a thermodynamic variable like external pressure has received less attention. The thermodynamic aspects of the glass transition, with a critical analysis of the available experimental data on the influence of pressure on T_g, has been discussed in detail by Goldstein [1]. Davis and Jones in their classic paper [2], derived an expression for the pressure dependence of T_g based on the hypothesis that the glass transition, although kinetically driven, occurs when some internal order parameter characterizing the thermodynamic state reaches a critical value. This relation is essentially the Ehrenfest relation for a second order transition viz.,

$$\frac{dT_g}{dP} = T_g V_g \frac{\text{Aa!}}{\Delta C_p} \tag{7.1}$$

Where $\Delta\alpha$ and ΔC_p are the discontinuities in the thermal expansion and the specific heat at the glass transition respectively.

An analogous relation can be derived using the discontinuities in the compressibility and thermal expansion.

$$\frac{dT_g}{dP} - \frac{\Delta K_T}{\text{Aa!}} \tag{7.2}$$

If the glass transition can be described using thermodynamics, then the ratio of the above two equations

$$\frac{T_g V_g (\Delta\alpha)^2}{\Delta C_p \Delta K_T} = 1 \tag{7.3}$$

Experimentally, it has been found that the R.H.S of the above equation is nearly 2 in most cases. According to Goldstein [1], this signifies that more than one order parameter is required to describe the glass transition.

The complete verification of the Ehrenfest relations requires the measurement of the specific heat, compressibility and the thermal expansion. Lot of work has been done in this direction []. In the present study, T_g has been measured as a function of pressure using Differential Thermal Analysis(DTA) and resistivity. This might yield useful information on the validity of the various models for the glass transition.

The resistivity measurements give us information on the variation of the mobility gap as a function of pressure. The change in the mobility gap at the glass transition has also been measured.

The chalcogenide glass chosen for the present study is $As_{40}Se_{30}Te_{30}$. Chalcogenide glasses are of interest to both to Physicists as well as technologists. Their technological importance is due to their use in the photonic industry, xerox machines etc. From a fundamental viewpoint they exhibit lot of interesting phenomena like electrical switching. Also, they form glasses over a wide range of compositions, so that the changes in the structure with change in co-ordination number can be studied. In chalcogenides, the phenomena of mechanical threshold and chemical ordering are well studied. Mechanical threshold or rigidity percolation occurs at an average co-ordination of 2.4, while chemical ordering occurs at an average co-ordination of 2.67. At a co-ordination of 2.4, the glass changes from a 2 dimensional network to a 3 dimensional covalent random network. The 3 dimensional structure is obviously more rigid than the 2 dimensional network and hence this phenomenon is known as rigidity percolation. The Chalcogenide glass chosen for our present study has an average co-ordination of 2.4 (the co-ordination numbers of As, Seand Te are 3,4 and 2 respectively). Hence this glass is exactly at the rigidity percolation threshold. According to the constraint counting theory of J.C.Phillips [3], the network becomes rigid when the number of degrees of freedom are exactly matched by the number of constraints on the system. The degrees of freedom correspond to the vibrational degrees of freedom, while the constraints are due to the bonds between the atoms in the network. Hence using the above condition, it can be shown rigorously that the condition for rigidity percolation is that the co-ordination number should be 2.4. Recently it has been shown [4] that the rigidity percolation might be shifted from 2.4 to a slightly higher value due to the presence of extra-degrees of freedom. Also, in glasses which have a sizeable percentage of Arsenic as in the present case, the

chemical ordering does not occur. This is due to the fact that $As - As$ homo-polar bonds are favoured, when compared to hetero-polar bonds. The two thresholds of rigidity percolation and mechanical ordering have significant effects on the electrical transport in these Chalcogenides [12]. Since in our study we have not measured the resistance as a function of pressure, we would not be seeing directly these effects. However the variation of the mobility gap as a function of pressure should also throw some light on these effects. Application of pressure changes the co-ordination number in the glass and hence one should see the effects of rigidity percolation and chemical ordering.

7.2 Differential Thermal Analysis

Differential Thermal analysis (DTA) is a widely used thermal technique for the detection of phase transitions. The basic principle of DTA is quite simple. The sample under study and the reference material (Alumina) are placed in small cavities which are located symmetrically with respect to the axis of a cylindrical cell (Fig. 7.1). The sample and reference temperatures are monitored using Chromel-Alumel thermocouples (in the present set-up). The entire DTA cell assembly is placed inside a furnace and heated at a constant rate. The reference material used should not undergo any transformations in the temperature range of interest. The temperature of the reference increases linearly with time, whereas the sample temperature will remain constant, when it is undergoing a first order transition. Therefore there will be a temperature difference between the sample and the reference. If this temperature difference (AT) is plotted as a function of the reference temperature, the transition point is seen as a peak or a trough depending upon whether the heat is liberated or absorbed by the sample during the transition. The area within the peak is proportional to the latent heat of the transition. Second order transitions are seen as a shift in the baseline, as there is a change in the specific heat at a second order transition.

Various criteria have been given for identifying the transition temperature from a DTA plot. For example the peak position can be taken as the transition temperature or the point where the trace of the temperature difference deviates from its constant value is identified as the transition temperature. There is a certain degree of arbitrariness in each of these criteria.

The important criterion to be fulfilled to get a 'good' DTA trace is that the sample and the reference material have to be thermally matched, i.e, the heat ca-

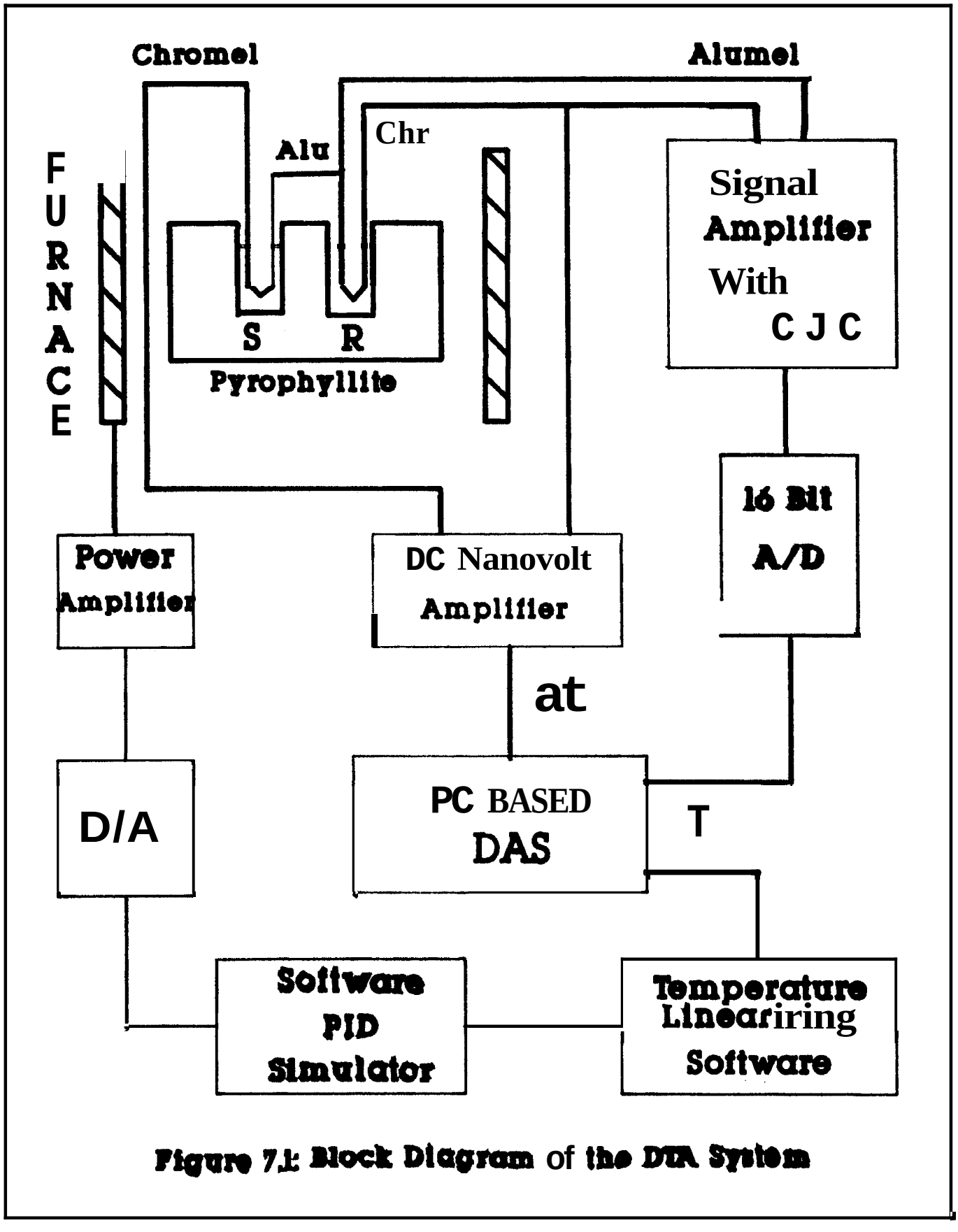

Figure 7.1: Block Diagram of the DTA System

pacity of the sample and the reference material have to be almost same. By a 'good' trace it is implied that even a very weak transition is easily detected. This can be achieved if a flat baseline is obtained. Otherwise the sample and reference temperatures will not increase at the same rate. The one having a higher heat capacity will heat up at a slower rate than the other giving rise to a baseline which is not flat. It is easier to detect small changes in AT, when the baseline is flat. To obtain a flat baseline the heat capacities are matched by adjusting the quantities of the sample and the reference. Trial runs are conducted and the quantity of the reference material is adjusted till a flat baseline is obtained. Certain problems are to be anticipated when this DTA technique is extended to higher pressures. The specific heat of the sample and the reference may change by different amounts when the DTA arrangement is pressurized. Hence even though, at atmospheric pressure, the sample and the reference may be thermally matched, a mismatch may develop at higher pressures. This effect will be seen when the results on the high pressure DTA measurements are discussed in later sections.

7.3 High Pressure DTA set up

The main component of the DTA set up used in the present investigation is the precision temperature programmer suitable for high pressure studies. Fig. 7.1 gives the block diagram of the temperature programmer coupled with the DTA cell used in the present studies. The system essentially consists of a high quality signal amplifier with automatic cold junction compensation (CJC), 16 bit A/D converter, a software for linearizing the thermo-emf versus temperature curve and implementation of the PID algorithm, a 16 bit D/A converter and a suitable power amplifier to provide the necessary power to the heating element. The signal amplifier consists of a differential input low-pass filter followed by an instrumentation amplifier (Burr Brown INA 101) configured for a gain of 200. The temperature transducer AD 592 which produces a voltage proportional to the temperature is used to provide automatic cold junction compensation for the Chromel-Alumel thermocouple. The amplified thermocouple voltage with CJC is digitized using a 16 bit A/D converter and a linearizing software transforms this signal directly to a value proportional to temperature. The software essentially fits a sixth order polynomial to the digitized thermo-emf. Since the effect of pressure on the thermo-emf of Chromel-Alumel is small, its use offers distinct advantages in high pressure studies. The fitting accuracy is $0.1^{o}C$ over the entire temperature range of 0-1000°C.

The design of the temperature controller is based on the well known PID type of control in a feed back loop. Care has to be taken so that the heater assembly and the sensing thermocouple are in good thermal contact.

The high temperature cell discussed in chapter 2 satisfies this important requirement. The PID algorithm computes in real time an error signal (difference between set point and actual temperature) which is the sum of a proportional gain, K_p, its integral and derivative terms K_i and K_D, respectively. A provision for fine tuning of these parameters facilitates good temperature control in the high pressure cells. The PID control signal is converted to a suitable analog signal using a 16 bit D/A converter. This analog PID signal is transformed to a power signal using a high voltage-high current operational amplifier. For controlling the temperature in the high pressure-high temperature cell, the power signal is used to control the current on the primary side of a step-down transformer whose secondary windings power the graphite heater. The step response of the temperature programmer is around 100 secs to reach stability for a step change of 100^o C. Temperature stability $\sim \pm 0.1^oC$ has been achieved. It is obvious that a temperature controller with a fast control action can be easily converted to a temperature programmer. If the set-point value in the PID algorithm is incremented linearly with time, the temperature of the sample will follow suit, provided the heating rate selected is slower than the rate of control action. Linear rate of heating/cooling which is software selectable , in the range 1 to 20^o C/minute has been achieved in the present set up. The DTA cell is machined out of Pyrophyllite with symmetrical bores to contain the sample and reference material like alumina. Chromel-Alumel thermocouples are in direct contact with the sample and reference and are brought out of the high pressure assembly through a four hole ceramic. The thermocouple signal from the reference chamber is used in the programmed heating of the cell assembly. The differential signal between the sample and the reference is amplified in a Keithley nanovolt amplifier (Model 181). Real-time digital filtering has been employed to improve the signal/noise ratio. The software has a provision for real-time plotting of the DTA signal as a function of temperature.

7.4 Sample preparation

Appropriate quantities (total 5 gms per batch) of high purity (99.999 %) As, Se and Te (from Koch Light Co.UK) were weighed into a fused silica ampoule (= 12 mm diameter). The contents were vacuum sealed under a pressure of 10^{-5} torr.

The ampoule was heated in a rotary furnace (for the purpose of homogenization) to 1000" C and after a couple of hours the temperature was reduced to 800^o C. The sample was kept in this condition for 20 hours, at the end of which the contents of the ampoule were quenched in ice cold water. The amorphous nature of the resulting material was confirmed using the X-ray diffraction technique.

7.5 Calibration of DTA apparatus

The DTA set-up was calibrated by using it to study some well-known transitions. The samples chosen for the calibration were Potassium Nitrate(KNO_3) and Indium(In).

From the literature, it is known that KNO_3 has a structural transition (orthorhombic to trigonal)at 129^o C and melts at 334 " C. The structural transition in KNO_3 can be easily located in the DTA curve (Fig. 7.2). From our studies, the transition temperature for the structural transition is determined to be 128.7" C. The melting point of Indium (156^o C), determined using the present set-up also matched with the literature values.

Fig. 7.3 shows the linear rate of heating (6" C/min) obtained using the DTA apparatus.

7.6 Results

Fig. 7.4 gives the DTA curve for the glass $As_{40}Se_{30}Te_{30}$ at ambient pressure. A heating rate of 10" C/minute was employed for these measurements. The sample was heated to a temperature beyond T_g at this rate and cooled at the same rate.

It may be noted that the glass transition manifests as a base line shift resulting from heat capacity changes near T_g. The supercooled liquid phase has a higher heat capacity than the glassy phase, as it has more degrees of freedom :- The translational degrees of freedom, which were frozen in the glassy phase, are available for excitation in the liquid phase. If the glass transition only results in a change in the specific heat, there will only be a shift in the baseline. However, near the transition , the specific heat rises to a maximum. This manifests as a minimum in the DTA curve (Fig. 7.4). The maximum in the specific heat hints at the critical dynamics, which takes place near the glass transition [5].

The value of T_g determined from this curve is around 135^o C and agrees well with the one determined from the standard DSC apparatus [6]. The thermogram at 5 kbar is given in Fig. 7.5. These experimental data were collected after the sample

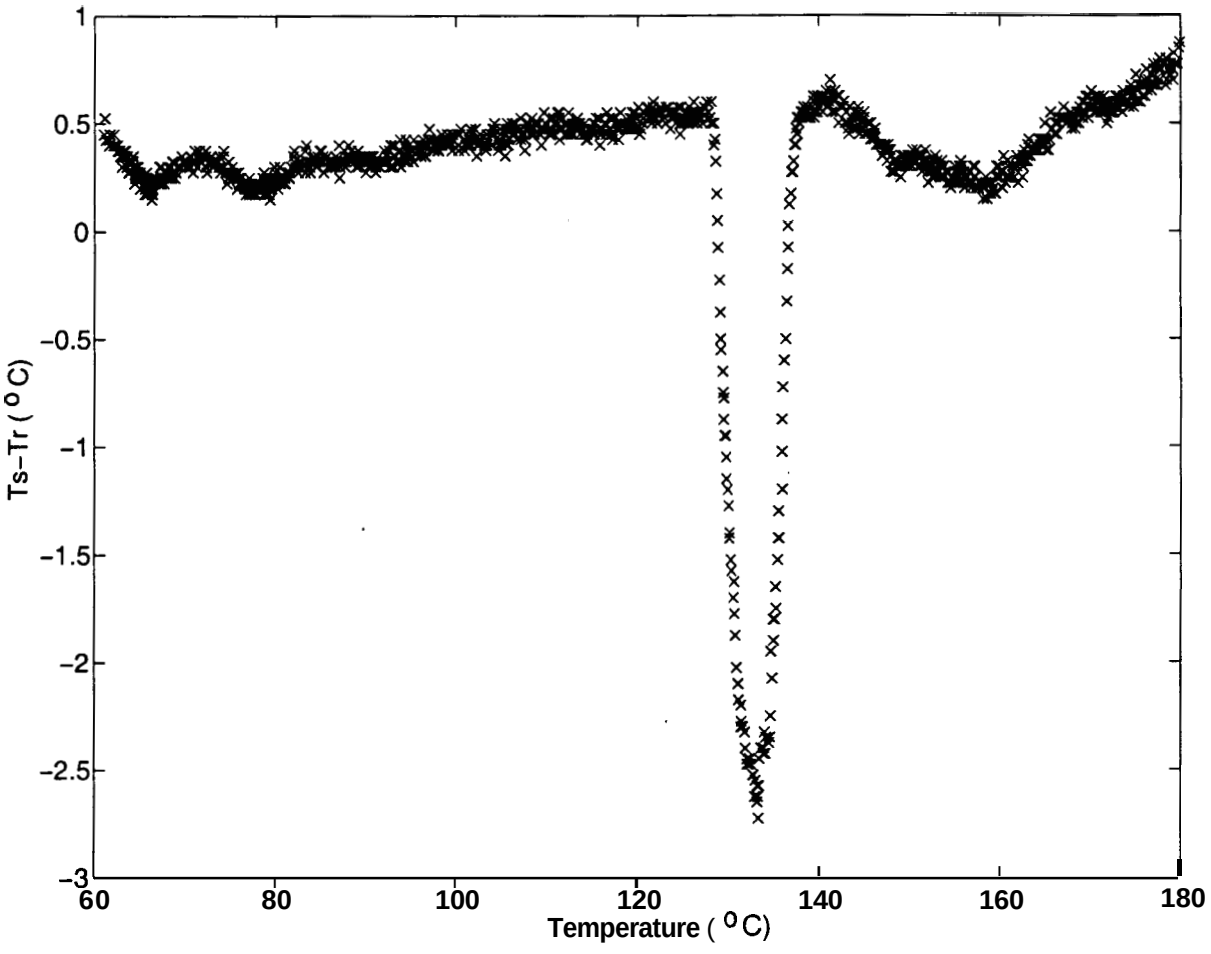

Figure 7.2: DTA trace for KNO_3, showing a structural transition around 129^o C.

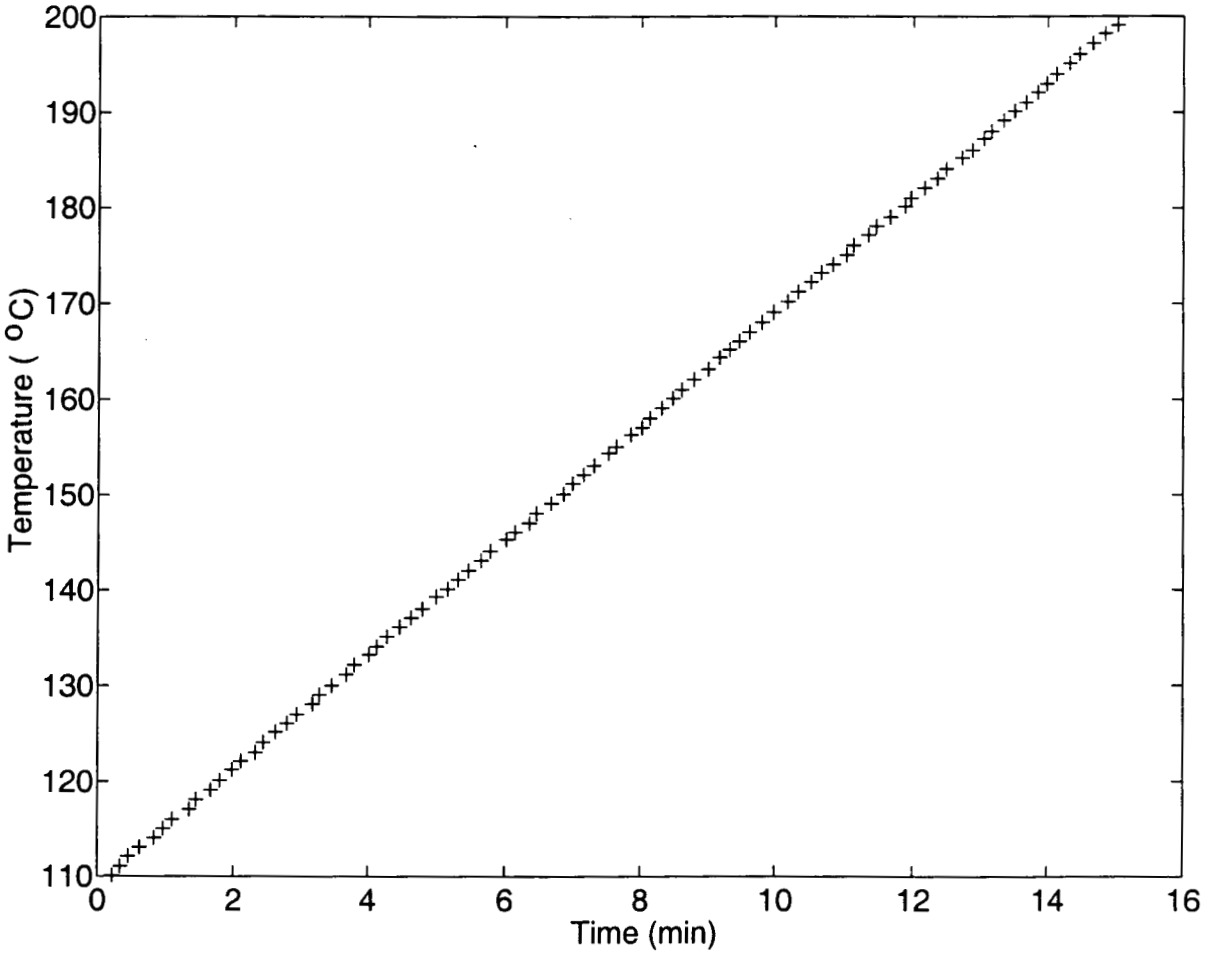

Figure 7.3: Linear rate of heating (6^o C/min) obtained using the DTA set-up.

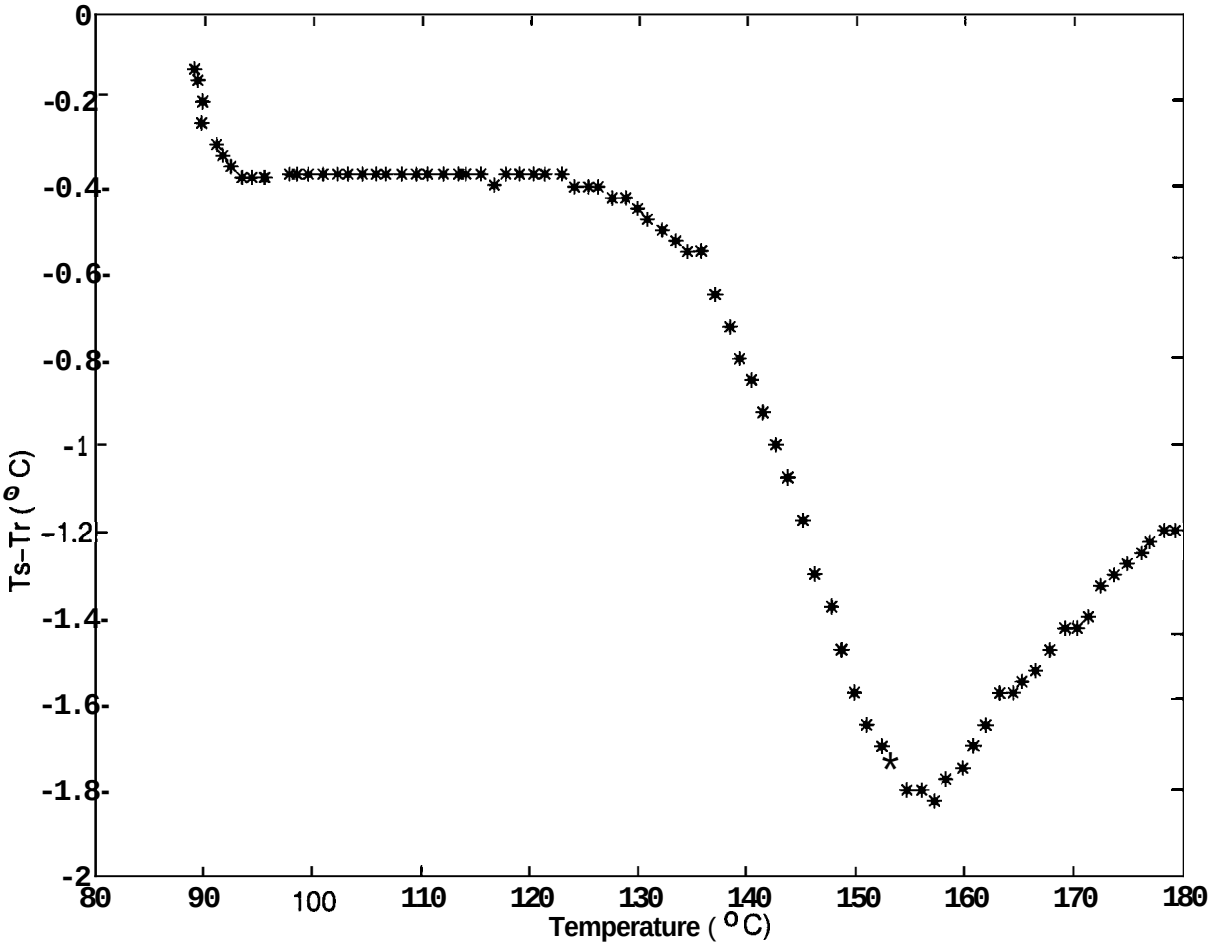

Figure 7.4: Typical DTA curve at ambient pressure

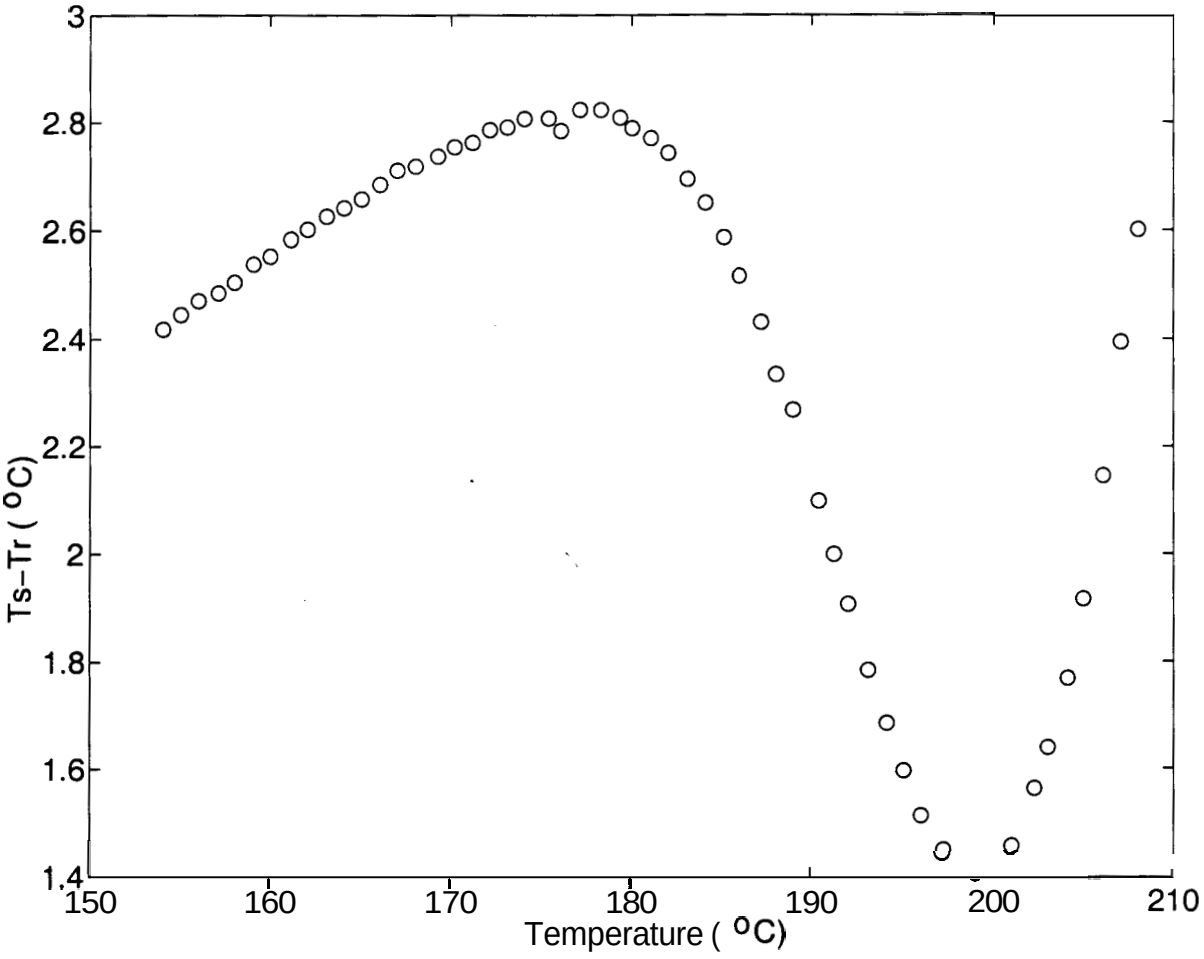

Figure 7.5: DTA of $As_{40}Se_{30}Te_{30}$ at 5 kbar

was pressurized in the glassy phase at a temperature much below T_g and subjected to a heating and cooling cycle at the same rate. The data obtained during the second heating run (Fig. 7.5) then corresponds to a glass with a well defined thermal history. It is well known that the glass transition temperature at high pressures depends on whether the sample is pressurized in the glassy phase or the liquid phase [7]. If the sample is pressurized in the liquid state which is highly compressible, the glass transition temperature and dT_g/dP is much higher.

It is clear that T_g has shifted to higher temperatures ($T_g \sim 180^oC$ at 5 kbar) compared to its value at room temperature. We also note that the base line becomes steeper at higher pressures due to the mismatch in the heat capacities of the sample and reference at higher pressures. However the anomaly near T_g is still discernable and the transition could be tracked up to 20 kbar, though at these pressures, T_g is

seen as just a slight change in the slope of the DTA curve (Fig. 7.6). The magnitude of the change in AT also seems to have reduced with pressure. This perhaps is indicative of a reduction in the change in specific heat $(\Delta C - \mathrm{p})$ at the glass transition with increasing pressure. A reduction in ΔC_p usually means that the glass is becoming "stronger". A "strong" glass is more disordered than a "weak" glass. This might be related to "pressure-induced amorphization".

High pressure experiments were carried out on this glass up to 20 kbar employing two different heating rates, viz., 5^o C/minute and 10" C/minute. The data on the shift of T_g with pressure are summarized in Fig. 7.7. Both the scan rates lead essentially to the same value of $dT_g/dP = 9^oC/kbar$. However the value of T_g at a particular pressure is higher if the heating rate is higher. The glass transition was also studied using resistivity techniques. The measurements were done at 5^o C/min and seem to agree well with the DTA measurements. The resistivity measurements will be discussed in detail in section. 7.8

7.7 Discussion

Experimental data on the pressure dependence of T_g in glass and polymer systems are scarce and mostly confined to pressure ranges lesser than **3** kbar. We believe that the present experimental results, where DTA signals in glasses could be tracked to 20 kbar and beyond are the first of its kind. The present results show that T_g increases linearly with pressure up to the highest pressures reached in these experiments. Further the magnitude of $dT_g/dP = 9^oC/kbar$ is of the same order as that observed in other systems like ionic liquids [8] and polymer systems [9].

The positive sign for dT_g/dP is consistent with the free volume model for the glass transition. According to the free-volume model [10], the glass transition occurs when the free-volume available in the liquid state, becomes insufficient to maintain the motion of the atoms or molecules and hence the atoms are frozen in their positions, leading to the glassy state. The free-volume increases with increase in temperature and reduces as the pressure is increased. Hence increasing the pressure, raises the glass transition temperature.

If we assume a thermodynamic description for the glass transition, then we can discuss the results for dT_g/dP on the basis of the Elirenfest relation:

$$\frac{dT_g}{dP} = \frac{TV\Delta C_p}{\Delta\alpha} \tag{7.4}$$

In the case of the glass transition, both ΔC_p and $\Delta\alpha$ are positive, since the

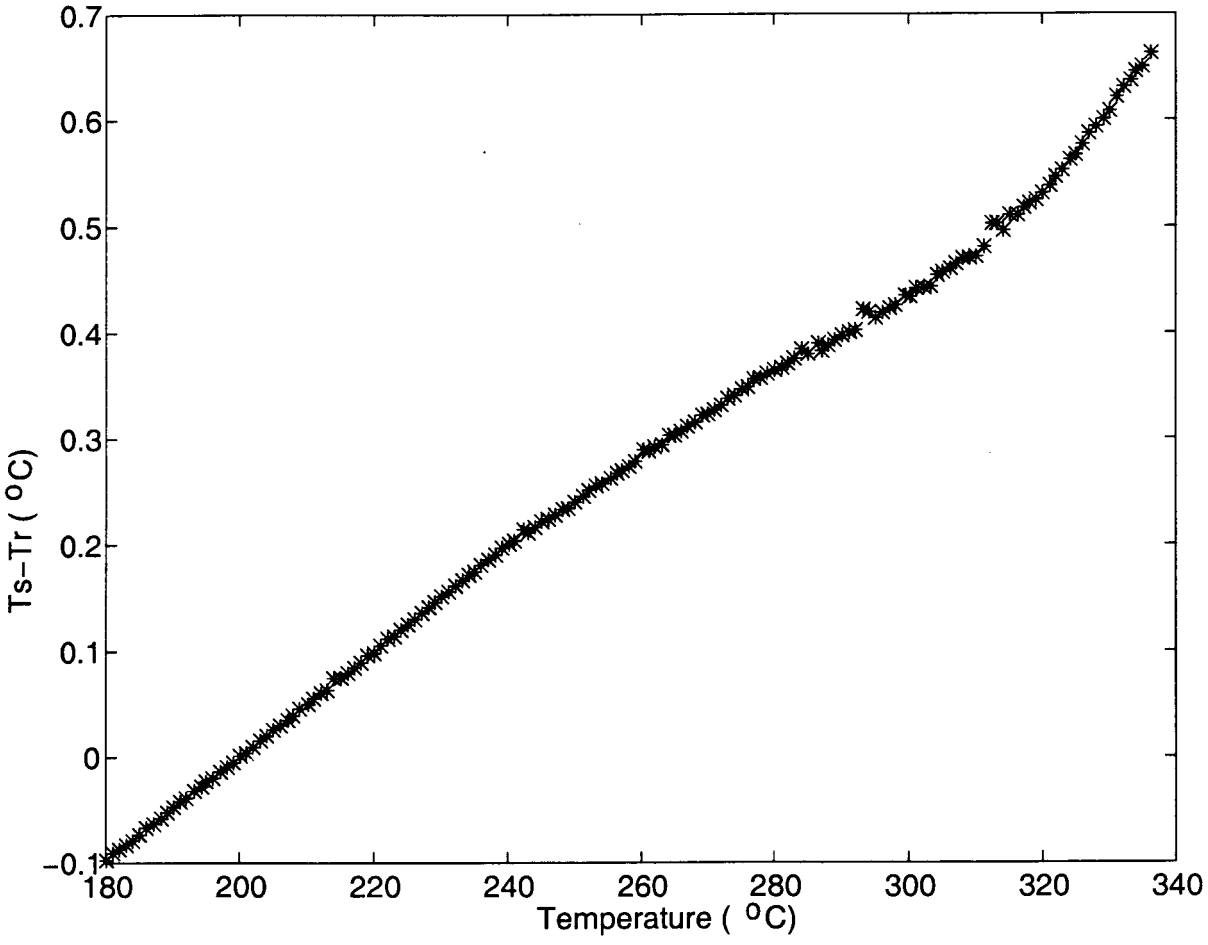

Figure **7.6: DTA of $As_{40}Se_{30}Te_{30}$ at 20 kbars.**

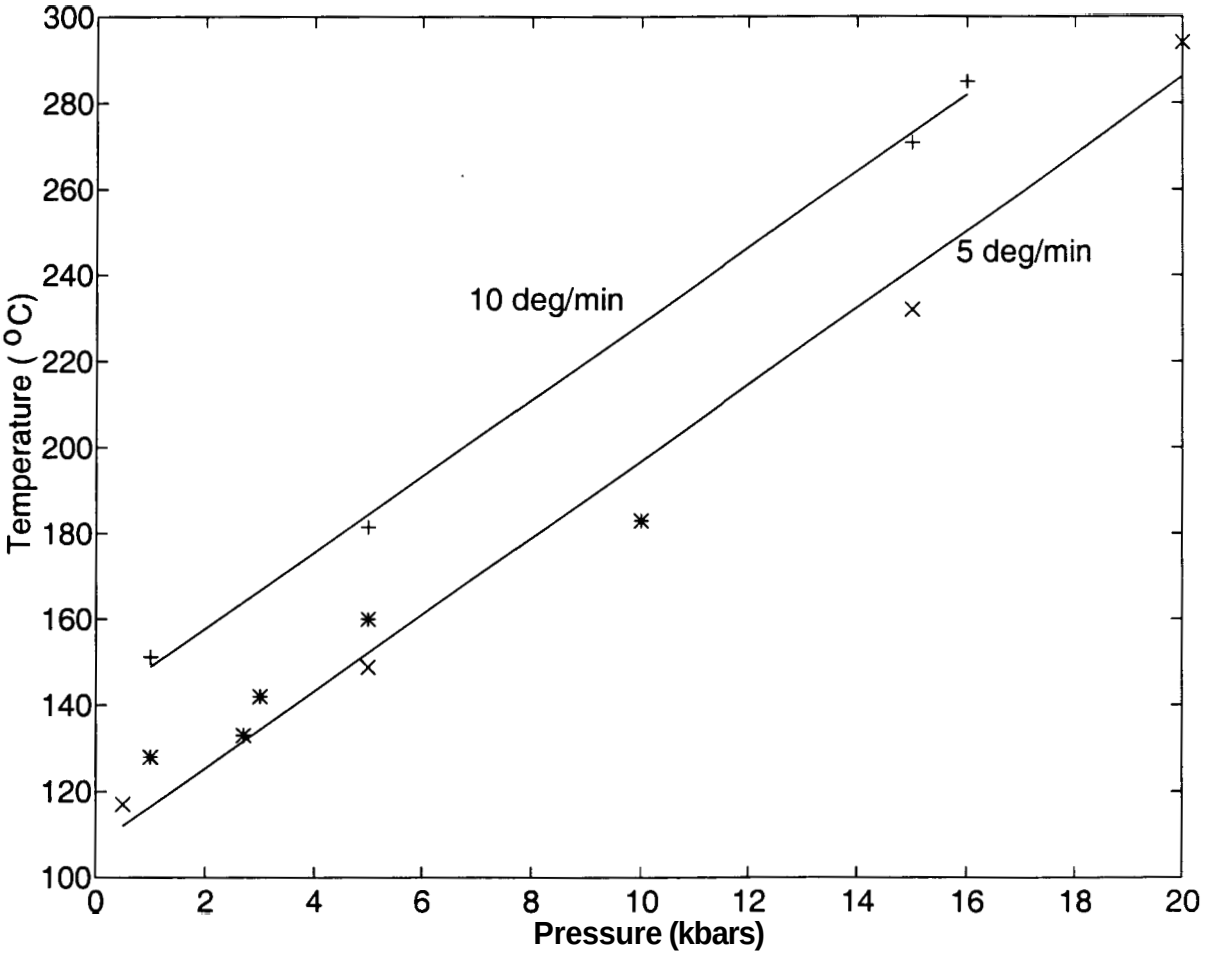

Figure 7.7: Pressure dependence of T_g for $As_{40}Se_{30}Te_{30}$ glass. '+'- *DTA* at 10^o C/min, 'x'- DTA at 5^o C/min and '*'- Resistivity at 5^o C/min

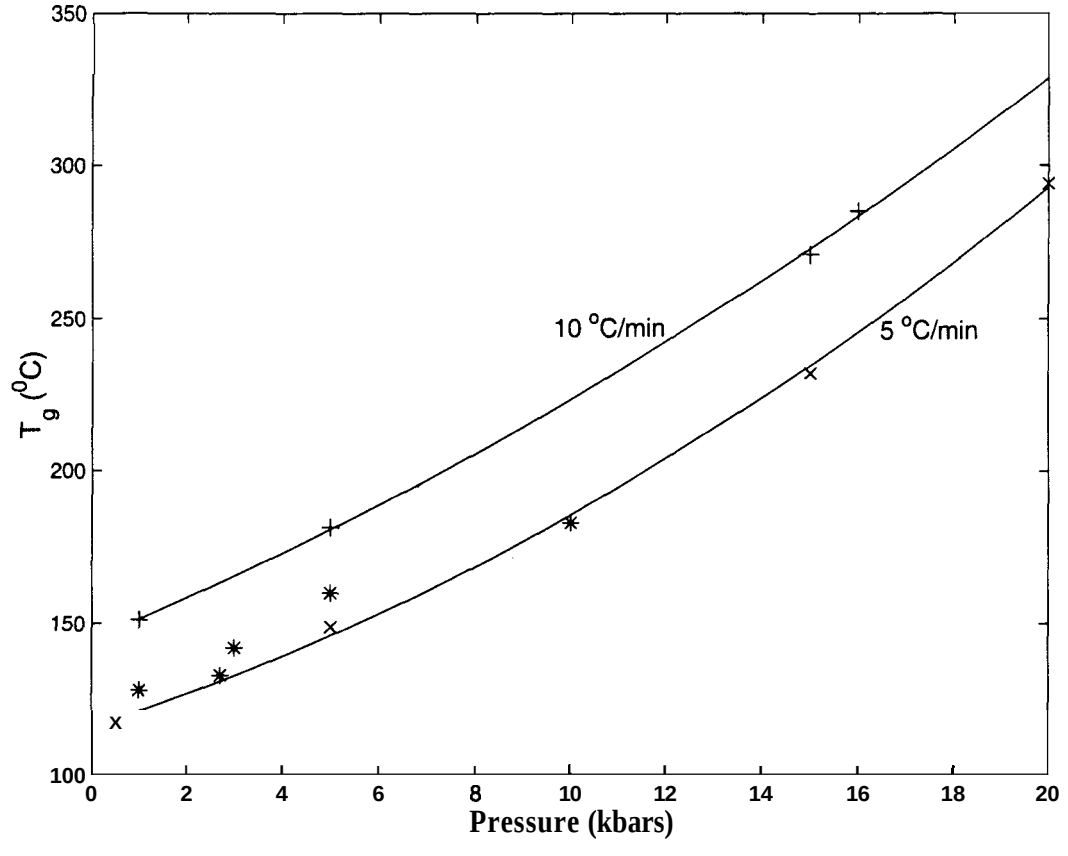

Figure 7.8: Pressure dependence of T_g for $As_{40}Se_{30}Te_{30}$ glass. '+'- *DTA* at 10^o C/min, 'x'- DTA at 5^o C/min and '*'- Resistivity at 5^o C/min. The lines show the quadratic fit to the data

---

liquid phase has a higher specific heat as well as a higher coefficient of thermal expansion.

Also if dT_g/dP is a constant (Fig. 7.7), the Ehrenfest implies that $\Delta C_p \propto \Delta\alpha$. Which means that the change in the heat capacity is entirely due to the change in the volume. However, in the case of the glass transition, the change in the heat capacity is also due to the extra translational degrees of freedom. Hence dT_g/dP should vary slightly with temperature. This might become apparent if the measurements are continued to higher pressures. Even in the present data, there is a small amount of non-linearity in the variation of T_g with pressure. It is seen from Fig. 7.8, that the data for T_g fits a second order polynomial better than a linear relation (Fig. 7.7). The coefficient of the second order term is of the order of 0.1 $^oC/kbar^2$, while the linear term is around 6 ^{o} C/kbar. If only a linear relation is fitted to the data $dT_g/dP \sim 9^oC/kbar$.

The glass transition temperature has also been related to the optical gap [11]. The idea is that the process of glass transition basically involves breaking of a number of bonds. The optical gap is proportional to the strength of the covalent bond. Hence T_g scales with the optical gap. However the linear relation between the gap and lnT_g is valid only for a particular average co-ordination number. With increase in the co-ordination number, the slope of $dlnT_g/dE_g$ increases [11]. From resistivity results (to be discussed in the next section), it is known that the energy gap reduces with increasing pressure. We have the paradoxical situation that while the gap is directly proportional to T_g, it decreases with pressure, eventhough T_g itself increases with pressure. This paradox can be resolved by assuming that the average co-ordination in the glass increases with pressure. There some evidence for this assumption. High pressure Electrical resistivity studies on Al-As-Te glasses [12] show certain certain anomalies which have been interpreted in terms of a change in the co-ordination number.

7.8 Electrical transport in chalcogenide glasses

The electrical transport properties of amorphous materials has certain new features when compared to their crystalline counterparts. Most of the additional features are due to the fact that the amorphous materials are completely disordered except for a short range order. Due to this the scattering in amorphous materials is more than for their crystalline counterparts. Due to this strong scattering, the mean free path is very short $(kL \sim 1)$, where k is the wave-vector of the electron and L is its mean-free path. It was first emphasized by Ioffe and Regel [13] that values of L such that $kL < 1$ are impossible. Hence the limit $kL = 1$ is known as the Ioffe-Regel limit. The Ioffe-Regel limit leads us to expect that, when the interaction of the charge carrier with atoms is sufficiently strong, something new ought to happen. It was first conjectured by Gubanov [14] and Banyai, that near the edges of conduction or valence bands in most non-crystalline materials, the states are localized, and the concept of localization plays a large part in the field of amorphous materials. The localized states are simply 'traps' and the most direct evidence for their existence in amorphous materials is provided by measurements of the transit time for injected carriers. If this shows an activation energy, a trap-limited mobility can be inferred. The new concept for amorphous amorphous materials is that a continuous density of states, $N(E)$, can exist in which for a range of energies the states are all traps, or in other words localized, and for which the mobility at the zero of temperature vanishes, even though the wave functions of neighbouring states overlap.

The first phenomenon for which this was generally recognized was impurity-conduction in doped and compensated semiconductors, which was first fully understood in the early 1960s. The impurity-centers in these materials are located at random positions, and in addition there is a random potential at each center. The understanding of localization in this case derives from Anderson's paper [15] on the "absence of diffusion in certain random lattices". In impurity conduction, each time an electron moves from one center to another, it emits or absorbs a phonon; processes in which it absorbs a phonon are rate-determining, and as a consequence the conductivity requires an activation energy, and it takes the form [16]:

$$\sigma = \sigma_o exp(-E_g/kT) \tag{7.5}$$

which tends to zero at low temperatures. This form of charge transport is called thermally activated hopping.

Energy values E_c and E_v separate the localized states from non-localized states. The energy difference $(E_c - E_v)$ defines a mobility gap E_g.

The pre-exponential factor a, in Eq. 7.5 is expected to be given by [16]:

$$\sigma_o \simeq 2.16e^2/z^2\hbar a_E \tag{7.6}$$

Where z is the co-ordination number and a_E is the average distance between the localized states.

A plot of $ln\sigma$ against 1/T will yield a straight line if $(E_c - \mathrm{E},)$ is a constant or if it is a linear function of T over the temperature range measured. If

$$E_c - E_v = E(0) - \gamma T \tag{7.7}$$

then the slope of such a plot will be $E(0)/k$, and the intercept will be In a, + (γ/k).

A striking difference between amorphous and crystalline semiconductors is that addition of atoms with valencies different from that of the host does not in general greatly affect the conductivity, i.e., they cannot be doped easily. The generally accepted explanation is that the disordered structure, including impurities, accommodates itself so that all the electrons are taken up in bonds. There is evidence that structural defects play a more effective role than do impurities in controlling the conductivity of amorphous semiconductors [18].

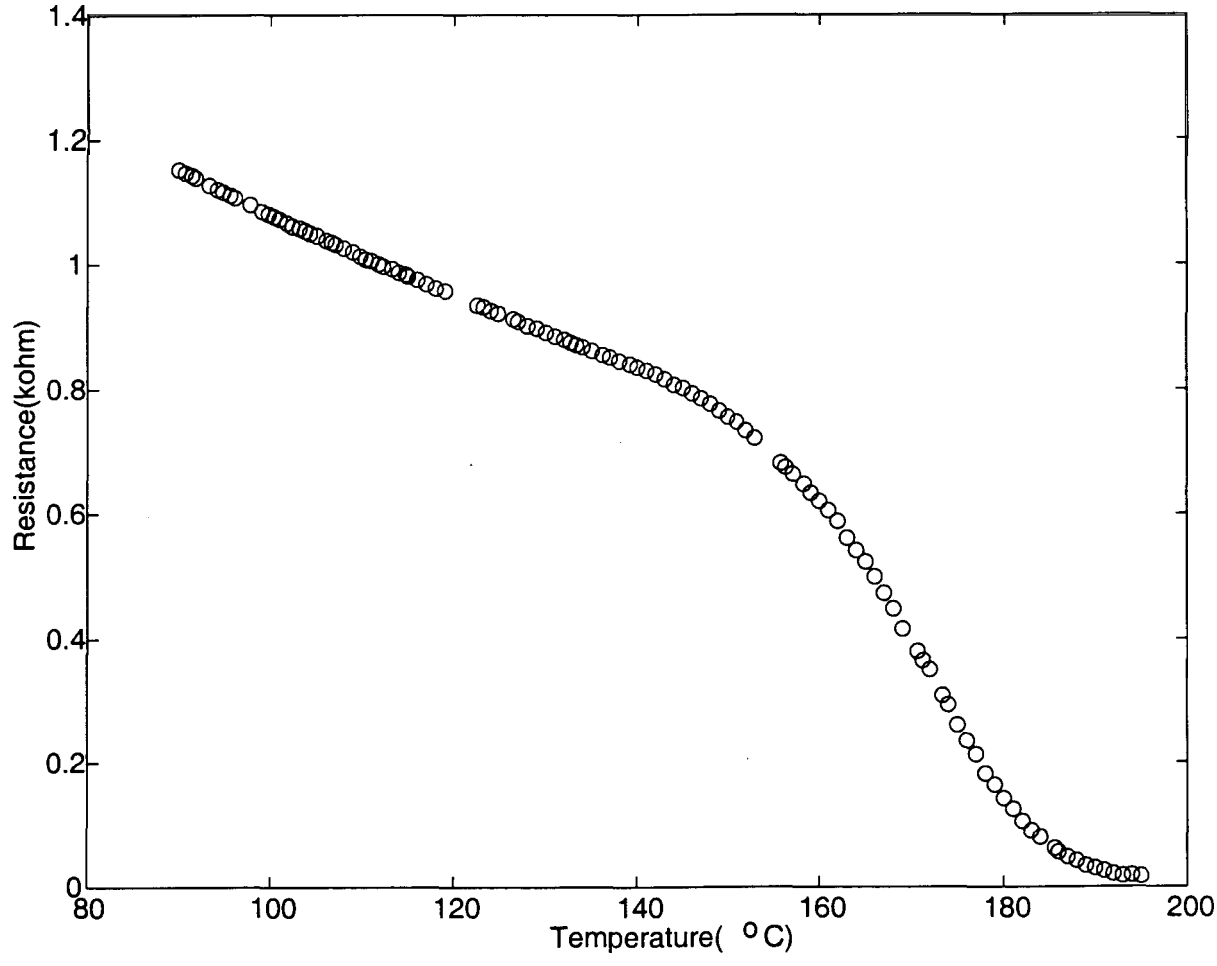

Figure 7.9: Resistance of $As_{40}Se_{30}Te_{30}$ as a function of temperature. The sharp decrease in resistance marks the glass transition.

7.9 Results

D.C. Resistivity studies were performed on $As_{40}Se_{30}Te_{30}$ using the standard 4-probe technique. The Keithley 2001 multimeter was used to make these measurements. The pressure was maintained at a constant value and the resistance was measured as a function of temperature. The conductivity of the sample (which is the inverse of the resistivity) roughly follows Eq. *7.5*.

The resistance of the sample is plotted as a function of temperature in Fig. *7.9*. There is a sudden decrease in the resistance around T_g. To determine whether the experimental data fits Eq. *7.5*, $ln\sigma$ is plotted against $1/T$ in Fig. *7.10*. There is an increase in slope at T_g. Such an increase in slope at T_g has been observed earlier in

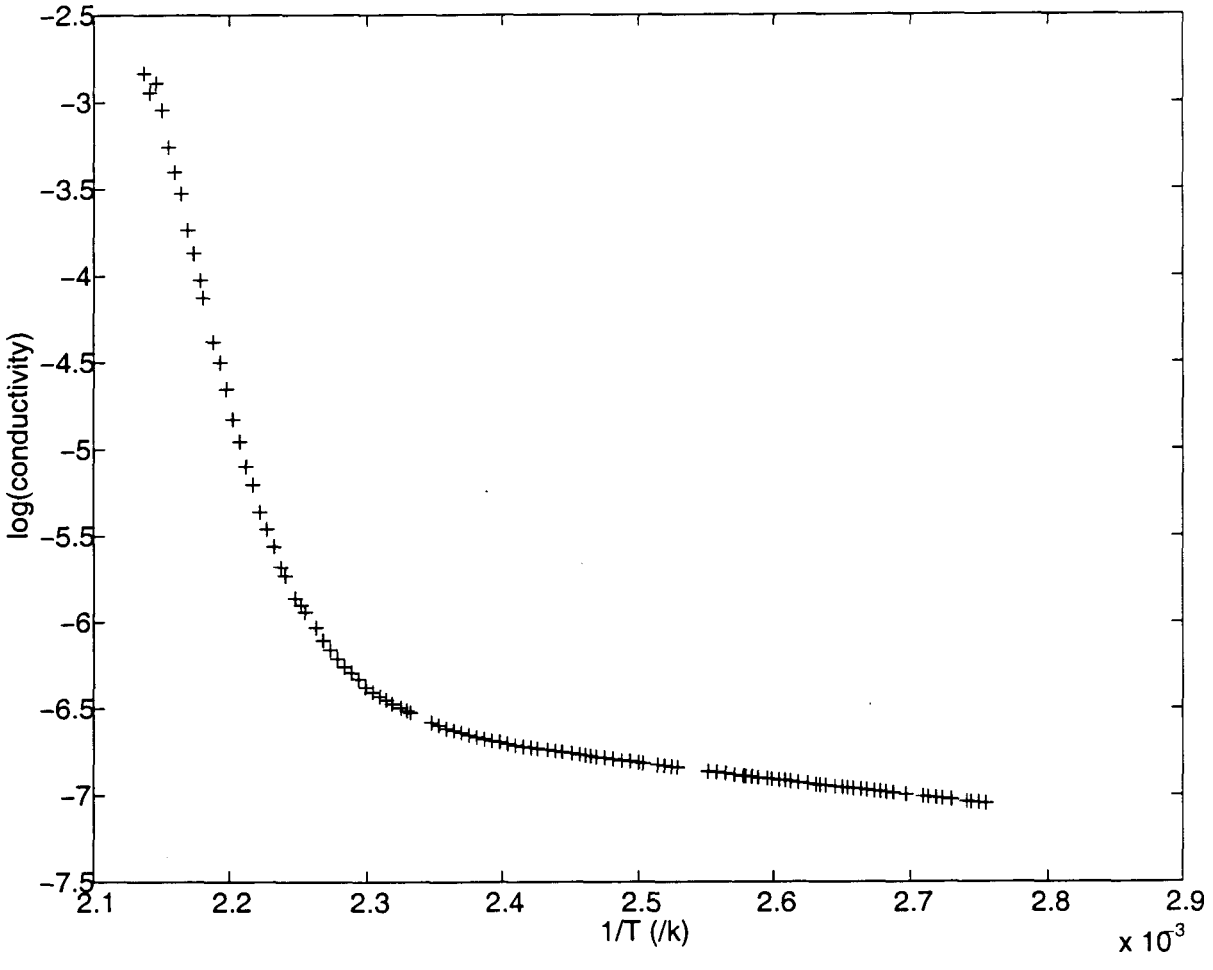

Figure *7.10:* Plot of $ln\sigma$ against $1/T$. T_g shows up as a change of slope in this plot.

---

the case of As_2Se_3 [17]. An increased slope suggests an increase in the temperature coefficient (y) of the activation energy. Thus the gap is decreased on going over to the liquid state.

The glass transition temperature can be determined either from the sharp decrease in the resistance or from the $ln\sigma - 1/T$ plot. T_g and $E(0)$ have been determined as a function of pressure and tabulated in table. *7.1.*

From the above table it is seen that the activation energy reduces sharply with pressure. However the rate of decrease in the gap with increasing pressure, is much more than what was determined in a previous study [18]. According to Geetha Ramani et al, the activation energy is 0.2 eV even at 60 kbar. Our results differ from these results since in each run, the glass is heated to a temperature above

Table 7.1: Glass transition temperature and activation energy as a function of pressure

Pressure (kbar)	$T_g(^oC)$	activation energy in eV(glass)	activation energy in eV(liquid)
1.1	128.0	0.28	0.84
2.7	133.0	0.40	0.84
3	142.0	0.84	1.5
5	160.0	0.08	0.6
10	183	0.003	0.17

T_g. Hence a new glass is formed at a high pressure, whose properties will be quite different from that of a glass formed at atmospheric pressure. In particular the density of this glass will be greater and its activation energy is much less than that of a glass formed at atmospheric pressure. Another puzzling feature is that the activation energy does not decrease monotonically as the pressure is increased. Instead it seems to have a maximum value around 3 kbar. The present experiments were done with a view to studying the variation of T_g as a function of pressure rather than for a determination of the activation energy. Reliable results on the activation energy as a function of pressure, can be obtained by maintaining the sample at a temperature below T_g and studying the variation in its resistivity as a function of pressure.

7.10 Conclusions

The glass transition temperature of $As_{40}Se_{30}Te_{30}$ has been measured as a function of pressure using DTA and resistivity. The pressure dependence of the activation energy has also been determined. The variation of T_g with pressure has been discussed in terms of the various models for the glass transition. A second-order polynomial seems to fit the variation of T_g with pressure.

References

[1] M. Goldstein J.Chem.Phys., 39, 3369 (1963)

[2] Davies and G.O.Jones, Adv.Phys.,**2**, 370 (1953)

[3] J.C.Phillips, J.Non.Cryst.Solids, 43, 37 (1981)

[4] R.A.Narayanan and A.Kumar, (To be published in Phys.Rev.B)

[5] Christoph Bennemann et al, Nature, 399, 246 (1999)

[6] Sudha Mahadevan and A. Giridhar, J.Non.Cryst.Solids, 221, 281 (1997)

[7] A.Angell, E.Williams, K.J.Rao and J.C.Tucker, J.Phys.Chem., 81, 238 (1977)

[8] Williams and C.A.Angell,J.Phys.Chem., **81**, 232 (1977)

[9] J.M.O'Reilly, J.Poly.Sci., **57** , 429 (1962)

[10] Richard Zallen, The Physics of amorphous solids, John Wiley and sons, 1983

[11] J.P.Neufille and H.K.Rockstad, 1,419, Proc. 5th *Int.Conf.Amorphous* and Liquid Semiconductors, Ed. J.Stuke and W.Brenig, Taylor and Francis, 1974

[12] M.Murali Mohan, Sudha Mahadevan and A.Giridhar, Pg. 153, Advances in High Pressure Science and Technology, Ed. A.K.Singh, Tata McGraw-Hill, New Delhi (1995)

[13] Ioffe, A.F. and Regel,A.R., Prog.Semicond., 4, 237 (1960)

[14] Gubanov,A.I., Quantum electron theory of amorphous conductors, Consultants Bureau, New York, 1965

[15] Anderson,P.W., Phys.Rev., **109**, 1492 (1958)

[16] N.F.Mott and E.A.Davis,Electronic Processes in Non-Crystalline Materials, Oxford University Press, London, 1971

[17] N.F.Mott and E.A.Davis, page 352 of *Electronic Processes in Non-Crystalline Solids,* Oxford University Press, London, 1971

[18] Geetha Ramani, A.Giridhar, A.K.Singh and K.J.Rao, Phil.Mag.B **39,385** (1979)